

# Gefitinib selectively inhibits tumor cell migration in *EGFR*-amplified human glioblastoma

Jonathon J. Parker, Kalen R. Dionne, Rada Massarwa, Marci Klaassen, Nicholas K. Foreman, Lee Niswander, Peter Canoll, B.K. Kleinschmidt-DeMasters, and Allen Waziri

Medical Scientist Training Program (J.J.P., K.R.D., A.W.), Departments of Cancer Biology (J.J.P., A.W.), Neuroscience (K.R.D.), Neurosurgery (M.K., B.K.K.-D., A.W.), Neurology (K.R.D., B.K.K.-D.), Pathology (B.K.K.-D.), and Pediatrics (R.M., N.K.F., L.N.), University of Colorado, School of Medicine, Anschutz Medical Campus, Aurora, Colorado; Howard Hughes Medical Institute (R.M., L.N.); The Children's Hospital Colorado, Aurora, Colorado (N.K.F.); and the Departments of Pathology and Cell Biology, Columbia University, New York, New York (P.C.)

**Background.** Tissue invasion is a hallmark of most human cancers and remains a major source of treatment failure in patients with glioblastoma (GBM). Although *EGFR* amplification has been previously associated with more invasive tumor behavior, existing experimental models have not supported quantitative evaluation of interpatient differences in tumor cell migration or testing of patient-specific responses to therapies targeting invasion. To explore these questions, we optimized an ex vivo organotypic slice culture system allowing for labeling and tracking of tumor cells in human GBM slice cultures. **Methods.** With use of time-lapse confocal microscopy of retrovirally labeled tumor cells in slices, baseline differences in migration speed and efficiency were determined and correlated with *EGFR* amplification in a cohort of patients with GBM. Slices were treated with gefitinib to evaluate anti-invasive effects associated with targeting *EGFR*. **Results.** Migration analysis identified significant patient-to-patient variation at baseline. *EGFR* amplification was correlated with increased migration speed and efficiency compared with nonamplified tumors. Critically, gefitinib resulted in a selective and significant reduction of tumor cell migration in *EGFR*-amplified tumors. **Conclusions.** These data provide the first identification of patient-to-patient variation in tumor cell migration in living human tumor tissue. We found that *EGFR*-

amplified GBM are inherently more efficient in their migration and can be effectively targeted by gefitinib treatment. These data suggest that stratified clinical trials are needed to evaluate gefitinib as an anti-invasive adjuvant for patients with *EGFR*-amplified GBM. In addition, these results provide proof of principle that primary slice cultures may be useful for patient-specific screening of agents designed to inhibit tumor invasion.

**Keywords:** *EGFR*, gefitinib, glioblastoma, invasion, migration, personalized therapy, slice culture.

Tissue invasion is a primary clinical concern in most human cancers. For patients with glioblastoma (GBM), treatment failure is attributable in many cases to diffuse infiltration of the surrounding normal brain, obviating curative surgical resection and limiting aggressive treatment with radiation therapy.<sup>1,2</sup> Despite extensive study of the mechanisms of GBM invasion, there are currently no clinically used therapies that effectively slow the spread of tumor cells. Clinical experience and biomathematical modeling of tumor growth kinetics from patient magnetic resonance imaging (MRI) indicate wide variations in rates of tumor dispersion.<sup>3</sup> In addition, recent genome-wide expression analyses have revealed multiple subtypes of GBM and have correlated differences in the activation of signaling pathways with response to therapy and prognosis.<sup>4,5</sup> Together, these data suggest that intrinsic variation of factors associated with tumor cell migration is inherent to GBM. These differences may mandate patient-specific selection of therapy to effectively target tumor invasion.

Received November 10, 2012; accepted March 7, 2013.

**Corresponding Author:** Allen Waziri, MD, Department of Neurosurgery, Academic Office Building One, Rm. 5001, 12631 E 17th Ave., Aurora, CO 80045 (allen.waziri@ucdenver.edu).

The underlying drivers of tumor cell movement are multifactorial. Both intrinsic and extrinsic forces are known to modulate glioma migration in the brain, although the relative contributions of nature (genetic and epigenetic characteristics of individual tumors) and nurture (nutrient supply and factors present in the tumor microenvironment) remain unclear. From a genetic standpoint, signaling through the epidermal growth factor receptor (*EGFR*) has been implicated as an activator of glioma cell motility.<sup>6–9</sup> On the environmental side, increasing evidence suggests that treatment-associated effects may alter the microenvironment and modulate the invasive behavior of tumors, as observed in the combined clinical experience with anti-angiogenic agents.<sup>10,11</sup> However, the a priori propensity for GBM to invade normal brain parenchyma on a patient-specific basis remains an ongoing area of study.

A variety of experimental paradigms have been previously used to study glioma cell migration. Prior studies exploring molecular mechanisms of glioma cell migration have documented differences between cells moving in the native brain extracellular matrix (ECM), compared with those migrating on rigid substrates in vitro, emphasizing the need for model systems that more faithfully recapitulate the in vivo architecture of human brain tissue.<sup>12,13</sup> The use of in vitro ECM models, transwell assays, or cells transplanted into normal animal brain slices, have been similarly limited.<sup>12–17</sup> Human orthotopic xenografts have been proposed to offer a closer representation of the human tumor microenvironment, but these models are complicated by incomplete penetrance for establishment of high-grade lesions, protracted growth periods, and loss of human stromal elements over time.<sup>18,19</sup>

We hypothesized that a model system using direct ex vivo organotypic slice cultures from freshly resected surgical specimens of human GBM would address these experimental limitations and allow for quantitative exploration of baseline differences in tumor cell migration among patients. Using this system, we evaluated the contribution of *EGFR* amplification to tumor migration and explored the potential patient-specific benefit of targeting *EGFR* to limit tissue invasion.

## Materials and Methods

### *Human GBM Organotypic Slice Culture Preparation and Retroviral Labeling*

Regulatory assurances, patient information, and methods associated with tissue harvesting are outlined in the Supplementary materials. Freshly resected human GBM specimens were embedded in low-melting temperature agarose (Invitrogen) and sliced into 350- $\mu$ m thick sections with a VT1000S Vibratome (Leica). Tumor-containing agarose blocks were processed while continuously submerged in media equilibrated with 95% O<sub>2</sub> and 5% CO<sub>2</sub>. Tumor slices were plated on 0.4- $\mu$ m pore hydrophilic PTFE inserts (Millipore) and maintained at 37°C in a humidified incubator with 5% CO<sub>2</sub>. Inserts were plated

on 1 mL of minimal media (Supplementary Materials) that was exchanged every 48 h. We found that the slice culture system, under minimal media conditions, provides sufficient trophic support for long-term culture while maintaining tissue viability, cellular constituency, and histological concordance with the originating tumor tissue (Supplementary Material, Fig. S1). To label tumor cells in GBM slices, we relied on retroviral tropism for dividing cells with use of a ZsGreen-expressing MMLV-based vector (Supplementary Materials). Tumor slices were infected and cultured for 72 h to allow for maximal expression of the fluorescent protein. For a subset of imaging experiments, Isolectin-IB<sub>4</sub> (a microglial binding lectin) conjugated to AlexaFluor 647 (Invitrogen) was added to the slice media at the concentration of 5  $\mu$ g/mL 2 h before imaging.

### *Evaluation of EGFR Amplification via Fluorescent In Situ Hybridization (FISH)*

FISH was undertaken to detect genomic amplification of the *EGFR* gene locus. Two dual-color chromosome enumeration assays for interphase cells were performed on formalin-fixed, paraffin-embedded tumor tissue that was pretreated with proteinase K and hybridized with a chromosome 7p12 (*EGFR*)-specific DNA probe and an alpha satellite probe for chromosome 7 centromere (Abbott Laboratories). Tumors were considered to be *EGFR* amplified if they contained populations of cells with >10 copies of *EGFR* per cell, based on 2 independent observers scoring 50 cells. All FISH and scoring were performed at the College of American Pathologists–certified Colorado Genetics Laboratory.

### *Time-Lapse Laser Confocal Microscopic Imaging of Labeled Human GBM Slices*

Tumor slices were transferred to nonlectin containing media before imaging in 1.5 thickness glass bottom dishes (MatTek). The slices were maintained at 37°C and 5% CO<sub>2</sub> in a sealed incubator (Pecon) on the microscope stage. An LSM 510 (Zeiss) confocal microscope equipped with a 10 $\times$  air objective (c-Apochromat NA 1.2) was used to image fields spanning a region between the slice edge and the center. The imaging depth varied from 150 to 250  $\mu$ m, with constant Z-step of 10  $\mu$ m and imaging interval of 11 min.

### *Tumor Cell Migration Path Tracking and Analysis*

Time-lapse confocal imaging data for each slice culture were preprocessed using Zen software (Zeiss) to make a maximum intensity projection through the depth of imaging, transforming 3-dimensional to 2-dimensional sequences. Manual cell-tracking was performed by one observer (J.J.P.) by marking the visually approximated center point of the ZsGreen-positive cell body (cell body centroid). Cell location was tracked approximately every 55 min. Tracking data were recorded using

ImageJ (NIH) and MTrackJ.<sup>20</sup> All cells with clearly visualized migration paths in one 10× field were tracked. Microglial cells that were both ZsGreen and Isolectin-IB<sub>4</sub> positive or had characteristic morphology were eliminated from subsequent analysis. Migration analysis was limited to those cells tracked at least 7.5 h and not stationary, defined as moving at least 10 μm (the approximate width of a tumor cell body) from their starting location. Cell track data were then analyzed in a defined coordinate system with use of Chemotaxis and Migration Tool V1.01 (Ibidi) to determine cell migration speed (μm/h), total path length (μm), and net path length (μm). Directionality was calculated using the ratio of net path length (μm) to total path length (μm). All calculated distances and subsequent speeds are an underestimate of actual values, which is inherent in the transformation of 3-dimensional images to 2-dimensional images.

### *GBM Slice Culture Treatment with Gefitinib*

Slice cultures were imaged for 11 h in vehicle control media (DMSO; 1:1000) and then switched to temperature and CO<sub>2</sub> pre-equilibrated media containing gefitinib at a concentration of 10 μM for another 11 h of imaging. Between control and gefitinib imaging periods, the culture insert was briefly removed from the imaging stage incubator, the media were changed, and the same imaging field was relocated. Identical imaging parameters were used for both imaging periods of the experiment, and cell tracking and filtration were performed as described above.

### *Statistical Analysis*

All statistical analysis was performed using Prism 5 (GraphPad). Data are presented as mean ± standard deviation unless otherwise noted. Significance was defined as a *P* value <.05. When significance was not reached, the *P* value is reported to indicate the strength of the statistic. When 2 groups of means were compared, a 2-tailed *t* test was used.

## Results

### *Significant Patient-to-Patient Variation Exists in the Invasive Behavior of GBM*

To explore intrinsic baseline differences in tumor cell migration in human GBM, we evaluated tumor cell migration parameters in organotypic slice cultures from a cohort of patients (Supplementary Material, Table S1). We limited sampling variability among patients by selectively obtaining tissue from the contrast-enhancing locations in the tumor (verified by intraoperative navigation). Slice viability at the time of imaging was confirmed through histopathological analysis, which demonstrated a general lack of necrosis or the appearance of pyknotic bodies (as determined by the senior neuropathologist on

the study, B.K.D.). In addition, staining for Ki67 at the time of imaging confirmed significant levels of ongoing cellular proliferation (mean, 28%; range, 5.5%–45%) across our cohort. Finally, minimal apoptosis was noted in late-stage slices as visualized by IHC for cleaved caspase-3 (Supplementary Material, Fig. S1).

For each tumor, individual migration paths were manually tracked in a single microscope field to generate a cell track map (Fig. 1A and B, Supplementary Material, Movie S1). Because the extent of brain invasion may be correlated on a macroscopic level with the relative burden of actively migrating cells, we initially generated a motility index for each patient specimen allowing for comparison of overall migratory activity among tumors. These ratios were calculated by comparing the number of cells actively migrating during the imaging period (moving at least a cell body's width, allowing for filtering of potential artifact-related micro-movement of the cell body throughout the imaging period) to the total number of fluorescent tumor cells in the imaging field. Calculated motility indices varied from 33% to 96% (mean ± standard deviation, 76% ± 18%) (Fig. 1C). Because the majority of tumors demonstrated motility indices >70%, baseline migratory activity on a cell-to-cell basis in most patients with GBM appeared to be fairly high.

To ascertain any tendency for unidirectional movement in slice cultures (ie, tropism, or the potential for all cells to migrate in a uniform direction) and to visualize cell dispersal, we centered the cell paths at a common starting point to create a displacement map (Fig. 1D). As expected, we observed no preferential directional movement of tumor cells in slices.

We next used time-lapse data to calculate cellular metrics of migration that would predictably contribute to the clinical behavior of tumors. Fundamentally, the migration of a cell is modified by 2 parameters: speed (distance travelled over time) and directionality (or efficiency, the dedication of a cell to a linear path during migration). To initiate the comparative analysis among tumors, migration speeds were obtained by averaging the distance traveled over time for individually tracked tumor cells. Mean migration speeds varied over a nearly 3-fold range in our cohort, spanning from 2.8 ± 1.9 μm/h to 7.8 ± 4.7 μm/h (Fig. 2A). We detected limited variability in cell migration speeds between separate slices from the same patient sample, confirming that differences observed between tumors were more likely related to intrinsic tumor-specific factors rather than conditions of culture.

The overall distribution of tumor cell speed in slice cultures displayed varying patterns on an inter-patient basis. Although most slices contained cells that were migrating faster than 5 μm/h (ranging from 7.4% to 78.3% across the cohort) (Fig. 2B), fewer tumors contributed slices with significant numbers of cells migrating faster than 10 μm/h (ranging from 1.1% to 28.6%) (Fig. 2C). Furthermore, as the mean speed for each tumor increased, the distribution of the cell speeds widened, as demonstrated by the positive correlation between mean speed and standard deviation ( $R^2 = 0.76$ ;  $P < .0001$ ). Together,

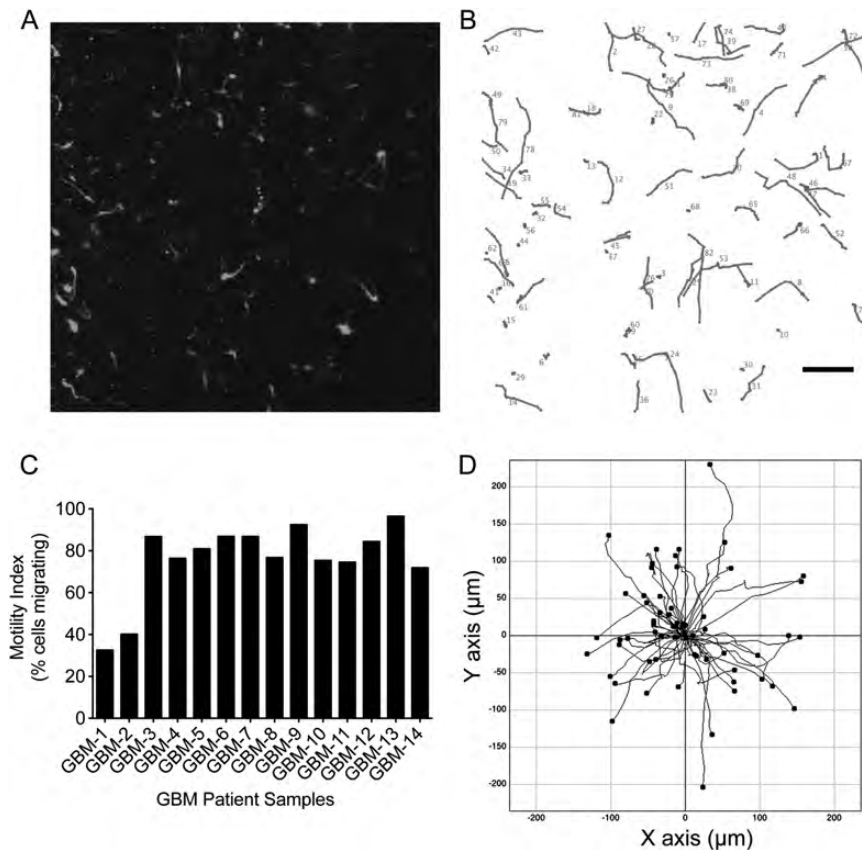


Fig. 1. Time-lapse confocal microscopy of tumor cells in human glioblastoma (GBM) slice cultures allows for tracking of cell migration in the tumor microenvironment. (A) Tumor cells expressing ZsGreen in human GBM slice cultures were visualized using confocal laser microscopy at 72 h after retroviral infection. A representative  $10\times$  microscope field is shown. (B) A migration path map was generated by tracking all tumor cells observed using the time-lapse images recorded from the tumor microregion in panel A. (C) The motility index, or percentage of cells that moved at least a cell width ( $10\ \mu\text{m}$ ) during the imaging, was calculated for each patient tumor cell population tracked ( $n = 14$ ). (D) A migration displacement map was generated by centering all tumor cell migration paths at a common starting point (scale is indicated on each axis).

these data indicate that tumors with higher mean speed harbor a subpopulation of fast tumor cells that are rare in tumors of lower mean speed and that the overall increase in mean speed is attributable to the presence of the faster population.

We next evaluated potential differences in the efficiency of tumor cell invasion among patients. Efficient migration (calculated as the migration directionality) requires that tumor cells demonstrate some level of persistence in their overall vector of movement (Fig. 2D). This biological metric may differ intrinsically among patient tumor cell populations and is predicted to exert significant effects on the overall rate of tumor cell invasion into the brain. To explore this hypothesis, we calculated and compared mean directionality quotients of labeled tumor cells in slices from our cohort of patients with GBM. As predicted, calculated values of mean tumor cell directionality varied significantly from patient to patient, ranging from  $0.43 (\pm 0.23)$  to  $0.81 (\pm 0.16)$  (mean,  $0.67 \pm 0.12$ ) (Fig. 2E).

Because both migration speed and efficiency contribute to the overall biological behavior of tumor cells, we next used a metric including both aspects of tumor cell movement to compare inter-patient differences in

invasion. The resulting effective migration speed, calculated as the accumulated average for the product of migration speed and directionality for each tumor cell, was determined for each patient in our cohort. Critically, mean effective migration speeds varied over a 7-fold range in this analysis (from  $0.92\ \mu\text{m}/\text{h}$  to  $6.7\ \mu\text{m}/\text{h}$ ) (Fig. 2F), confirming significant heterogeneity in effective tumor cell migration among patients and providing a possible physiologically relevant *in vitro* correlate for observed clinical differences in tumor invasion.

#### EGFR Amplification Is Associated with Augmented Migration in GBM

Amplification of the *EGFR* gene is present in  $\sim 40\%$  of primary human GBM and has been previously associated with infiltrative behavior.<sup>7,9,21–23</sup> Although prior work has suggested that the invasive front of tumor growth is enriched with *EGFR*-amplified cells<sup>22</sup> and comparative MRI analysis has implied that *EGFR*-amplified tumors exhibit increased tumor invasion,<sup>24</sup> a direct correlation between *EGFR* amplification and increased metrics of migration on a cellular basis has not been shown with human

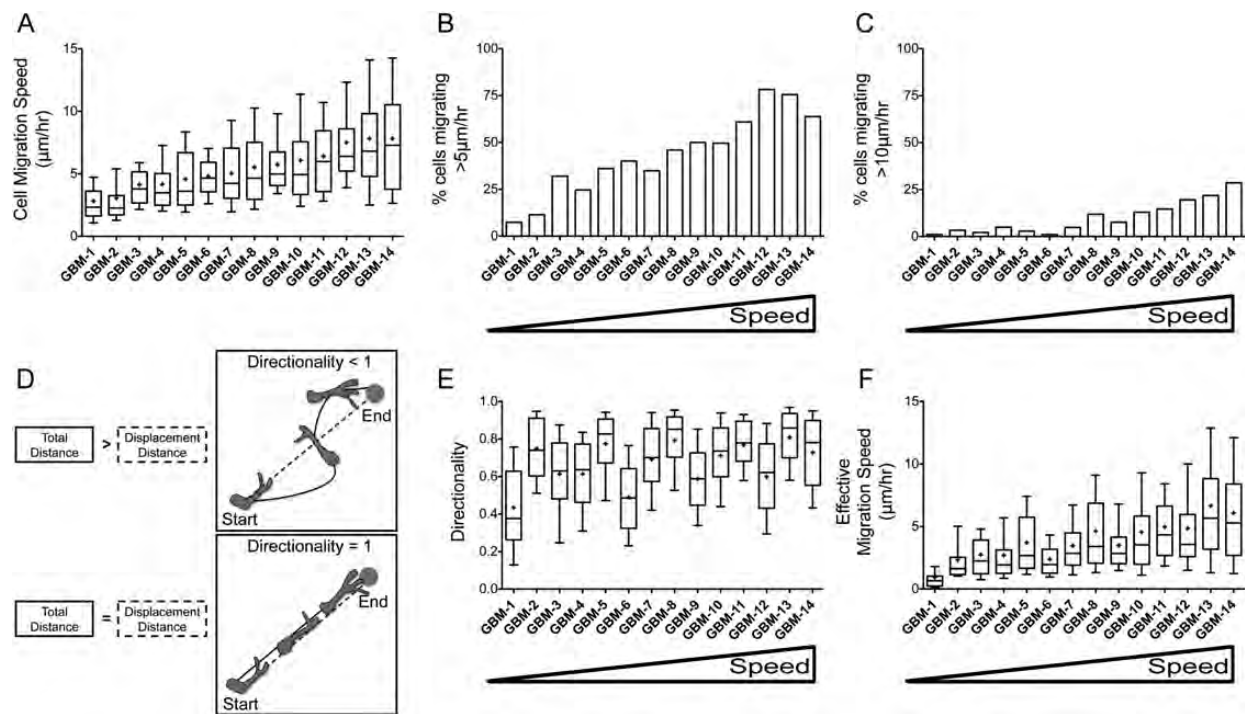


Fig. 2. Heterogeneity exists in tumor cell migration speed, directionality, and effective migration speed among patients with glioblastoma (GBM). (A) Cell migration speed varied significantly across our cohort of tracked tumor cell populations ( $n = 14$ , ANOVA  $P < .0001$ ). Bars represent the speed of the 10th to 90th percentile cells, the line represents the median, and the cross represents the mean cell migration speed of the tumor cell population. (B) The percentage of cells migrating faster than  $5 \mu\text{m}/\text{h}$  varied among tumor cell populations. Tumor cell populations from patients with GBM are ordered left to right according to increasing mean cell migration speed. (C) In a subset of tumor cell population, there was an increased number of cells that migrated faster than  $10 \mu\text{m}/\text{h}$ . (D) Graphical representation of the migration directionality, depicting cells with less efficient (top, directionality  $< 1$ ) and more efficient (bottom, directionality = 1) patterns of migration. (E) Directionality of tumor cell migration within organotypic slices varied significantly among patients ( $n = 14$ , ANOVA  $P < .0001$ ). (F) Effective migration speed varied  $\sim 7$ -fold across our patient cohort ( $n = 14$ , ANOVA  $P < .0001$ ).

GBM. We therefore attempted to directly correlate *EGFR* amplification in donor tumor tissue specimens with migration characteristics of tumor cells in organotypic slices. Tumor cells in slices from *EGFR*-amplified patients trended strongly toward greater mean speed ( $6.1 \pm 1.5 \mu\text{m}/\text{h}$ ) than did tumor cells from nonamplified patients ( $4.8 \pm 1.6 \mu\text{m}/\text{h}$ ;  $P = .14$ ) (Fig. 3A), and *EGFR* amplification was significantly associated with increased mean directionality ( $0.73 \pm 0.07$ ), compared with nonamplified tumors ( $0.61 \pm 0.11$ ;  $P < .05$ ) (Fig. 3B). Perhaps of most importance, effective migration speed was significantly increased in *EGFR*-amplified tumors ( $4.6 \pm 1.4 \mu\text{m}/\text{h}$ ), compared with nonamplified tumors ( $3.0 \pm 1.1 \mu\text{m}/\text{h}$ ;  $P < .05$ ) (Fig. 3C). Together, these data provide critical and physiologically relevant support for the hypothesis that *EGFR* amplification is associated with augmented cell migration in human GBM.

#### Targeting *EGFR* with Gefitinib Selectively Decreases Tumor Cell Migration in *EGFR*-Amplified Tumors

Given confirmatory data that *EGFR*-amplification is associated with increased intrinsic migratory behavior in human GBM, we hypothesized that targeting the activity

of this receptor would selectively affect tumor cell movement in receptor-amplified tumors. We chose to use the small molecule tyrosine kinase inhibitor gefitinib for these purposes, because this drug has been previously tested in early trials of GBM and is widely used on a clinical basis for other systemic cancers.<sup>25–27</sup>

Control and gefitinib-treated time windows were generated from slices for each tested patient. To visualize the effect of gefitinib on cell migration across tumor slices on a macroscopic level, we again created displacement maps showing the effective dispersal distance of each tracked cell in the population. A substantial qualitative decrease was observed in cell dispersion in *EGFR*-amplified tumors after treatment with gefitinib, whereas no differences were noted in the *EGFR*-nonamplified tumors (Fig. 4D, E, and Supplementary Material, Movie S2).

On a quantitative level, treatment of *EGFR*-amplified tumors resulted in a mean decrease in mean speed of  $2.3 \mu\text{m}/\text{h}$  ( $6.1 \pm 1.6 \mu\text{m}/\text{h}$  to  $3.8 \pm 0.7 \mu\text{m}/\text{h}$ ), whereas mean speed in nonamplified tumors displayed a negligible mean change of  $0.3 \mu\text{m}/\text{h}$  ( $4.6 \pm 1.5 \mu\text{m}/\text{h}$  to  $4.3 \pm 1.5 \mu\text{m}/\text{h}$ ) (Fig. 4A). Minimal effects were noted in either population with regard to tumor cell directionality after gefitinib treatment (Fig. 4B). However, treatment of *EGFR*-amplified tumors resulted in a

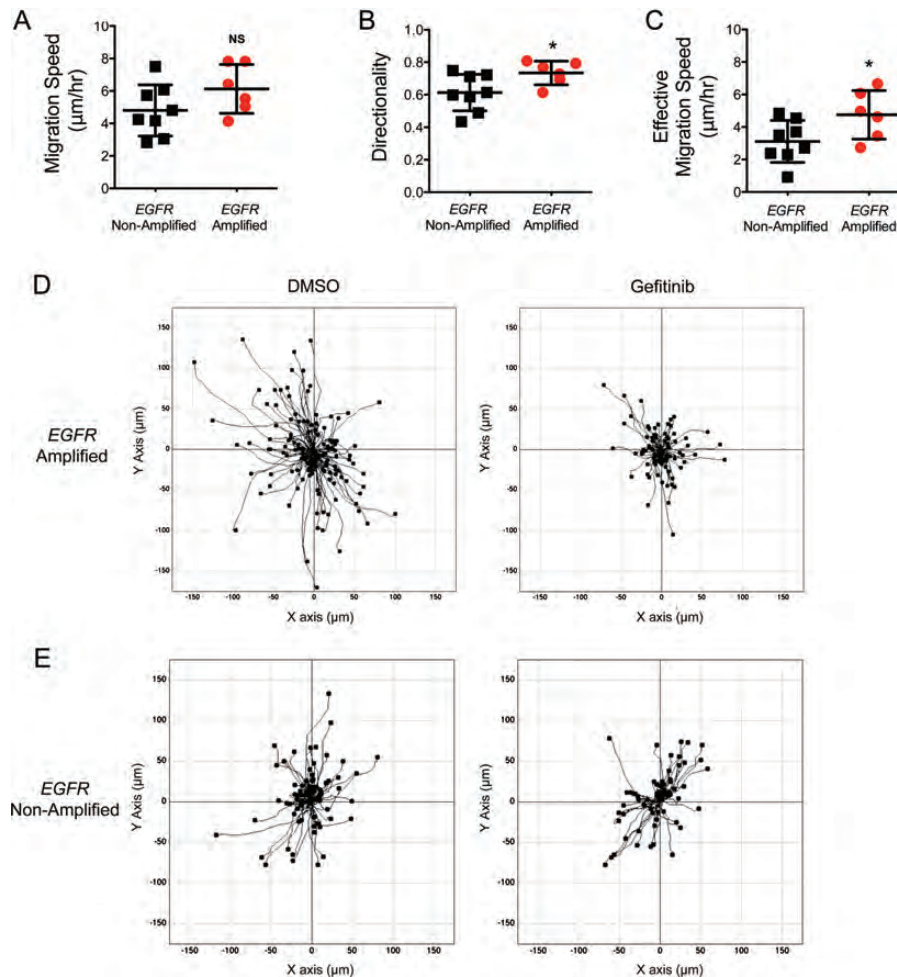


Fig. 3. *EGFR* amplification is associated with augmented migration in human glioblastoma (GBM), and selective targeting of *EGFR* reduces tumor cell migration in receptor-amplified patients. Comparison of mean migration speed (A), directionality (B), and effective migration speed (C) among *EGFR*-amplified and nonamplified tumors. Directionality and effective migration speed were significantly increased in amplified tumors ( $P < .05$  for both metrics), whereas migration speed trended toward an increase in amplified tumors ( $P = .14$ ). (D) Representative displacement maps generated during imaging of pretreated (DMSO) and posttreated (gefitinib) conditions, demonstrating differential qualitative effects of *EGFR* inhibition on tumor cell migration in slices from *EGFR*-amplified (D) and nonamplified (E) GBM.

significant decrease in effective migration speed of  $2.1 \mu\text{m/h}$  ( $4.8 \pm 1.3 \mu\text{m/h}$  to  $2.7 \pm 0.7 \mu\text{m/h}$ ), whereas negligible changes were seen in nonamplified tumors (Fig. 4C).

Because *EGFR* amplification occurs in a subset of cells from each tumor, we hypothesized that the fast-moving populations in amplified tumors represent the individual cells with *EGFR* amplification. Therefore, we predicted that gefitinib would selectively target the subset of faster migrating cells in slices from amplified tumors. To explore this possibility, we stratified individual cell populations in slices into  $5 \mu\text{m/h}$  bins. Analysis of cell speed distribution demonstrated that gefitinib treatment decreased the number of cells migrating faster than  $5 \mu\text{m/h}$  in *EGFR*-amplified tumors by a mean of 33% (shifting the majority of remaining migrating cells below  $5 \mu\text{m/h}$ ), whereas a minimal change was seen in nonamplified tumors (Fig. 4D and E), confirming that the drug may have a selective effect on the subpopulation of faster migrating tumor cells. Critically, gefitinib treatment did

not completely ablate tumor cell migration in any of the *EGFR*-amplified tumors, but rather reduced mean migration speeds to levels commensurate with the nonamplified tumors ( $3.8 \pm 0.7 \mu\text{m/h}$  vs  $4.6 \pm 1.5 \mu\text{m/h}$ ).

## Discussion

Future success in the treatment of GBM will likely derive from disruption of tumor infiltration into previously uninvolved brain tissue. Because the invasive behavior of GBM is known to be markedly heterogeneous,<sup>3,5,28</sup> exploration of baseline characteristics of tumor cell migration on a patient-to-patient basis will be critical for determining prognosis, predicting response to treatment, and testing efficacy of various targeted therapies. In addition, the ability to disrupt migration of tumor cells will be particularly relevant in combination with locally aggressive or anti-angiogenic therapy, because these

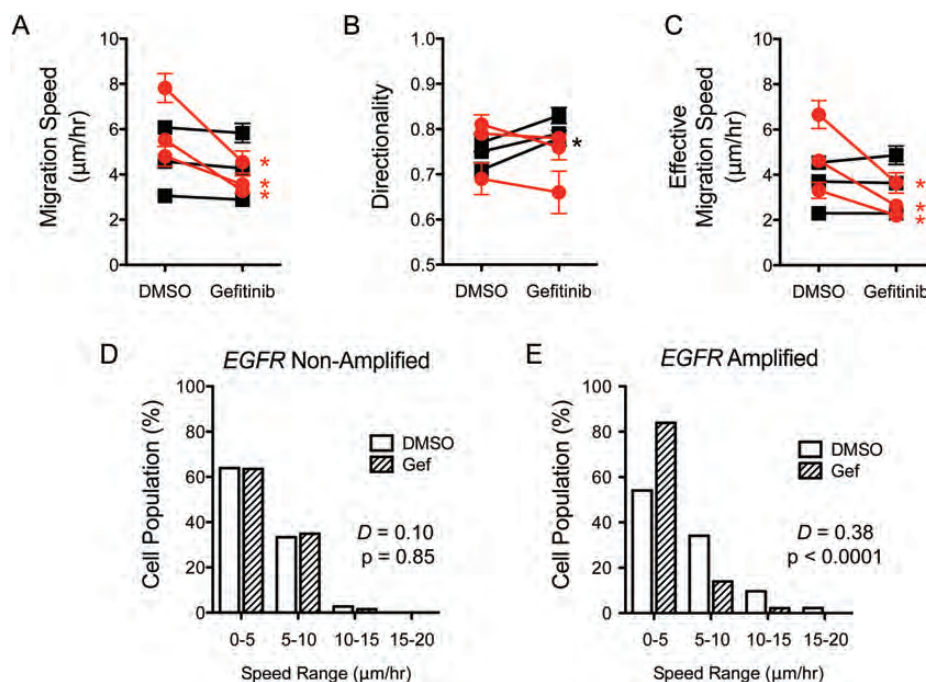


Fig. 4. Gefitinib exhibits selective effects on tumor cell migration in *EGFR*-amplified glioblastoma (GBM). Quantitative analysis of the effects of gefitinib on mean migration speed (A), directionality (B), and effective migration speed (C) for *EGFR*-amplified (red circles) and nonamplified (black squares) tumors. Mean migration speed and effective migration speed significantly decreased in each *EGFR*-amplified tumor with treatment ( $P < .02$  for all tumors), whereas no decrease was observed in nonamplified tumors. One *EGFR*-nonamplified tumor demonstrated a significant change in directionality ( $P = .005$ ). Error bars represent standard error of the mean (SEM). Representative analysis of tumor cells in nonamplified (D) and amplified (E) tumors before (DMSO) and after gefitinib (Gef) treatment, subdivided by migration speed into 5  $\mu\text{m/h}$  bins, confirming selective dropout of faster migrating cells after treatment in *EGFR*-amplified tumors. Analysis of each of these tumor cell populations before and after gefitinib treatment via the Kolmogorov-Smirnov test demonstrated the *EGFR*-amplified cell population had a significant ( $P < .0001$ ) shift in the distribution of cell population speeds, whereas the *EGFR*-nonamplified population demonstrated no shift ( $P = .85$ ).

manipulations have been recently suggested to augment the invasive behavior of targeted tumor cells.<sup>10,11,29–31</sup>

Although prior experimentation has explored a range of factors associated with increased tumor invasion in GBM,<sup>13,17,32–34</sup> these studies have been somewhat limited in providing physiological relevance to the human system. The organotypic slice culture system offers an *ex vivo* approach allowing for relative maintenance of the tumor microenvironment in an *in vitro* setting. Of note, external nurture elements can be held constant or manipulated at will (through the controlled application of oxygen, glucose, and other nutrients). Using this system, we have confirmed that characteristics of tumor cell migration differ significantly on a patient-to-patient basis under matched macroenvironmental conditions. These results provide *in vitro* support for the observed heterogeneity in GBM invasion and the contribution of intrinsic nature-based factors (ie, genetic or epigenetic), unique ratios of microenvironmental cellular constituencies, or tumor-specific alterations of extracellular matrix in driving these differences.

A number of investigators have previously explored the role of *EGFR* as a potential driver of migratory behavior in GBM. Aghi et al. noted that patients with *EGFR*-amplified GBM exhibit a significantly higher

ratio of T2/T1 signal on MRI (a surrogate for diffuse tumor invasion) compared with nonamplified patients.<sup>24</sup> These observations were further supported through studies documenting the increased prevalence of *EGFR*-amplified cells at the infiltrative edge of human GBM, compared with the hypercellular core of the tumor mass.<sup>21,22</sup> Prior *in vitro* studies have suggested that *EGFR* signaling increases directional persistence of glioma cell migration,<sup>8,35</sup> and forced overexpression of *EGFR* via retroviral transduction of white matter progenitors in the rodent brain leads to increased numbers of highly migratory cells.<sup>36</sup> Using the slice culture system, we have for the first time, to our knowledge, provided direct quantitative correlation between *EGFR* amplification and increased tumor cell migration in human GBM. Because GBM slices with higher mean migration speed and efficiency appear to harbor subpopulations of faster cells that are responsible for driving the overall mean migration behavior upward, we hypothesize that this phenomenon is related to the known heterogeneity of *EGFR* amplification on an intra-patient basis and that faster migrating cells are, in fact, the subpopulation of *EGFR*-amplified cells. Although live-imaging conditions required for migration analysis in the slice model have prohibited attempts to confirm this hypothesis using

formal immunohistochemical methods, observations from the gefitinib treatment experiments provide indirect support. Of note, treatment of *EGFR*-amplified slices with gefitinib results in a selective dropout of the faster migrating cells, reducing the overall migration characteristics of tumor cells in these slices closer to those recorded from nonamplified specimens.

The small group of clinical trials targeting *EGFR* in GBM have generally documented limited therapeutic benefit. In 3 of the largest phase II protocols using gefitinib in either primary or recurrent tumors, a lack of significant survival advantage was seen when compared with historical controls.<sup>25–27</sup> In all trials with gefitinib treatment, *EGFR* amplification did not correlate with clinical response to gefitinib in post-hoc analysis,<sup>25,26</sup> although in each of these settings, a small fraction of long-term responders were noted (which may be related to PTEN status<sup>37</sup>). Critically, therapeutic efficacy of targeting *EGFR* in these trials has specifically focused on traditional outcome measures, such as progression-free or overall survival. Because *EGFR* amplification is not thought to be an oncogenic driver of human GBM, it remains unclear what therapeutic benefit should be expected by targeting this pathway in affected patients. On the basis of data from the slice model, we would propose that specific targeting of patients with *EGFR*-amplified tumors and the use of alternate outcome measures (eg, effects on expansion of nonenhancing infiltrative tumor) may expose potential benefits of *EGFR* inhibitors that were not seen in prior clinical trials. We conjecture that combination therapy with more traditional antineoplastic agents could decrease tumor invasion into normal brain tissue, which is a primary source of treatment failure in many patients. Of note, effective penetration of drugs into tumor tissue remains an area of concern. Prior work in mouse models of glioma has indicated that distribution of gefitinib into the tumor and associated brain parenchyma may be limited by several mechanisms, including cellular drug efflux pumps.<sup>38</sup> Studies of human GBM tissue from patients receiving gefitinib demonstrate at least a 10-fold drug concentration according to tumor to plasma ratio.<sup>25,39</sup> However, in a study of drugs concentrations in tissue from patients undergoing treatment, the mean concentration of intratumoral gefitinib was  $\sim 1.7 \mu\text{M}$  (assuming a tumor density of 1 g per mL), which is within a comparable pharmacological range to the concentration used in the current study.<sup>39</sup>

Although the organotypic slice model offers many opportunities for physiologically relevant study of tumor cell migration in human GBM, there remain several limitations with this experimental approach. Slice cultures retain many critical elements of the tumor microenvironment; however, the system does not provide for a continuous blood supply, maintenance of macro-level 3-dimensional architecture of the human brain (including long-range white matter tracts, grey-white matter boundaries, or large caliber vessels), or the continually shifting nutrient, growth factor, and chemokine milieu that would be present in the living human brain. Because of

constraints associated with live imaging of slices, we have not yet developed a technical approach allowing for histochemical or genetic analysis of individual cells determined to be moving faster or slower in slices. Such analysis will be critical for further direct definition of genetic or protein expression patterns associated with increased migration in the heterogeneous background of GBM. Furthermore, it is well known that regional differences in GBM genetics occur on an intra-tumoral basis, indicating that cellular heterogeneity may contribute to observed differences in cell migration rates.<sup>21</sup> Perhaps most importantly from a translational perspective, our experiments do not yet provide a direct causative link between increased ex vivo cell migration speed and/or directionality seen in tissue slices and the extent of tumor invasion and clinical outcome in human GBM. Ongoing studies using an increased number of slices with more detailed protein and genetic analysis will help to further define these relationships.

At present, there remain no clinically available agents designed to target tumor invasion in human GBM. Although a number of candidates have been proposed, the ability to test these agents in a patient-based and physiologically relevant system will be critical for establishing overall efficacy and, more importantly, allowing for personalization of therapy in this highly heterogeneous disease. The organotypic slice model potentially offers an ideal platform for these purposes because drugs can be tested in relatively rapid fashion after initial tumor resection (<2 weeks). Future studies using the slice model for testing anti-invasive agents and correlation with targeted clinical trials will be instrumental in further defining the potential translational use of this model.

## Supplementary Material

Supplementary material is available at *Neuro-Oncology Journal* online (<http://neuro-oncology.oxfordjournals.org/>).

## Acknowledgments

We thank members of the University of Colorado Department of Neurosurgery for their collaboration in the collection of patient tumor tissue samples and Dr. James DeGregori for contributing gefitinib for these studies.

*Conflict of interest statement.* None declared.

## Funding

This work was supported by the American Cancer Society, the Cancer League of Colorado, the Neurosurgery Research and Education Foundation, and the family of Lisa Ann Miller.

## References

- Gaspar LE, Fisher BJ, Macdonald DR, et al. Supratentorial malignant glioma: patterns of recurrence and implications for external beam local treatment. *Int J Radiat Oncol Biol Phys.* 1992;24(1):55–57.
- Sanai N, Polley MY, McDermott MW, Parsa AT, Berger MS. An extent of resection threshold for newly diagnosed glioblastomas. *J Neurosurg.* 2011;115(1):3–8.
- Wang CH, Rockhill JK, Mrugala M, et al. Prognostic significance of growth kinetics in newly diagnosed glioblastomas revealed by combining serial imaging with a novel biomathematical model. *Cancer Res.* 2009;69(23):9133–9140.
- Verhaak RG, Hoadley KA, Purdom E, et al. Integrated genomic analysis identifies clinically relevant subtypes of glioblastoma characterized by abnormalities in *PDGFRA*, *IDH1*, *EGFR*, and *NF1*. *Cancer Cell.* 2010;17(1):98–110.
- Phillips HS, Kharbanda S, Chen R, et al. Molecular subclasses of high-grade glioma predict prognosis, delineate a pattern of disease progression, and resemble stages in neurogenesis. *Cancer Cell.* 2006;9(3):157–173.
- Feng H, Hu B, Jarzynka MJ, et al. Phosphorylation of dedicator of cytokinesis 1 (Dock180) at tyrosine residue Y722 by Src family kinases mediates *EGFR*III-driven glioblastoma tumorigenesis. *Proc Natl Acad Sci USA.* 2012;109(8):3018–3023.
- Guillamo JS, de Bouard S, Valable S, et al. Molecular mechanisms underlying effects of epidermal growth factor receptor inhibition on invasion, proliferation, and angiogenesis in experimental glioma. *Clin Cancer Res.* 2009;15(11):3697–3704.
- Kim HD, Guo TW, Wu AP, Wells A, Gertler FB, Lauffenburger DA. Epidermal growth factor-induced enhancement of glioblastoma cell migration in 3D arises from an intrinsic increase in speed but an extrinsic matrix- and proteolysis-dependent increase in persistence. *Mol Biol Cell.* 2008;19(10):4249–4259.
- Martens T, Laabs Y, Gunther HS, et al. Inhibition of glioblastoma growth in a highly invasive nude mouse model can be achieved by targeting epidermal growth factor receptor but not vascular endothelial growth factor receptor-2. *Clin Cancer Res.* 2008;14(17):5447–5458.
- de Groot JF, Fuller G, Kumar AJ, et al. Tumor invasion after treatment of glioblastoma with bevacizumab: radiographic and pathologic correlation in humans and mice. *Neuro-oncology.* 2010;12(3):233–242.
- di Tomaso E, Snuderl M, Kamoun WS, et al. Glioblastoma recurrence after cediranib therapy in patients: lack of “rebound” revascularization as mode of escape. *Cancer Res.* 2011;71(1):19–28.
- Ulrich TA, de Juan Pardo EM, Kumar S. The mechanical rigidity of the extracellular matrix regulates the structure, motility, and proliferation of glioma cells. *Cancer Res.* 2009;69(10):4167–4174.
- Beadle C, Assanah MC, Monzo P, Vallee R, Rosenfeld SS, Canoll P. The role of myosin II in glioma invasion of the brain. *Mol Biol Cell.* 2008;19(8):3357–3368.
- de Bouard S, Christov C, Guillamo JS, et al. Invasion of human glioma biopsy specimens in cultures of rodent brain slices: a quantitative analysis. *J Neurosurg.* 2002;97(1):169–176.
- Nygaard SJ, Haugland HK, Laerum OD, Lund-Johansen M, Bjerkvig R, Tysnes OB. Dynamic determination of human glioma invasion in vitro. *J Neurosurg.* 1998;89(3):441–447.
- Palfi S, Swanson KR, De Bouard S, et al. Correlation of in vitro infiltration with glioma histological type in organotypic brain slices. *Br J Cancer.* 2004;91(4):745–752.
- Ling J, Liu Z, Wang D, Gladson CL. Malignant astrocytoma cell attachment and migration to various matrix proteins is differentially sensitive to phosphoinositide 3-OH kinase inhibitors. *J Cell Biochem.* 1999;73(4):533–544.
- Ogden AT, Waziri AE, Lochhead RA, et al. Identification of A2B5+CD133- tumor-initiating cells in adult human gliomas. *Neurosurgery.* 2008;62(2):505–514; discussion 514–505.
- Kopetz S, Lemos R, Jr, Powis G. The promise of patient-derived xenografts: the best laid plans of mice and men. *Clin Cancer Res.* 2012.
- Meijering E, Dzyubachyk O, Smal I, van Cappellen WA. Tracking in cell and developmental biology. *Semin Cell Dev Biol.* 2009;20(8):894–902.
- Snuderl M, Fazlollahi L, Le LP, et al. Mosaic amplification of multiple receptor tyrosine kinase genes in glioblastoma. *Cancer Cell.* 2011;20(6):810–817.
- Okada Y, Hurwitz EE, Esposito JM, Brower MA, Nutt CL, Louis DN. Selection pressures of TP53 mutation and microenvironmental location influence epidermal growth factor receptor gene amplification in human glioblastomas. *Cancer Res.* 2003;63(2):413–416.
- Furnari FB, Fenton T, Bachoo RM, et al. Malignant astrocytic glioma: genetics, biology, and paths to treatment. *Genes Dev.* 2007;21(21):2683–2710.
- Aghi M, Gaviani P, Henson JW, Batchelor TT, Louis DN, Barker FG, 2nd. Magnetic resonance imaging characteristics predict epidermal growth factor receptor amplification status in glioblastoma. *Clin Cancer Res.* 2005;11(24 Pt 1):8600–8605.
- Hegi ME, Diserens AC, Bady P, et al. Pathway analysis of glioblastoma tissue after preoperative treatment with the *EGFR* tyrosine kinase inhibitor gefitinib—a phase II trial. *Mol Cancer Ther.* 2011;10(6):1102–1112.
- Rich JN, Reardon DA, Peery T, et al. Phase II trial of gefitinib in recurrent glioblastoma. *J Clin Oncol.* 2004;22(1):133–142.
- Uhm JH, Ballman KV, Wu W, et al. Phase II evaluation of gefitinib in patients with newly diagnosed Grade 4 astrocytoma: Mayo/North Central Cancer Treatment Group Study N0074. *Int J Radiat Oncol Biol Phys.* 2011;80(2):347–353.
- Diehn M, Nardini C, Wang DS, et al. Identification of noninvasive imaging surrogates for brain tumor gene-expression modules. *Proc Natl Acad Sci USA.* 2008;105(13):5213–5218.
- Ebos JM, Kerbel RS. Antiangiogenic therapy: impact on invasion, disease progression, and metastasis. *Nat Rev Clin Oncol.* 2011;8(4):210–221.
- Keunen O, Johansson M, Oudin A, et al. Anti-VEGF treatment reduces blood supply and increases tumor cell invasion in glioblastoma. *Proc Natl Acad Sci USA.* 2011;108(9):3749–3754.
- Lu KV, Chang JP, Parachoniak CA, et al. VEGF inhibits tumor cell invasion and mesenchymal transition through a MET/VEGFR2 complex. *Cancer Cell.* 2012;22(1):21–35.
- Assanah MC, Bruce JN, Suzuki SO, Chen A, Goldman JE, Canoll P. PDGF stimulates the massive expansion of glial progenitors in the neonatal forebrain. *Glia.* 2009;57(16):1835–1847.
- Ivkovic S, Beadle C, Noticewala S, et al. Direct inhibition of myosin II effectively blocks glioma invasion in the presence of multiple motogens. *Mol Biol Cell.* 2012;23(4):533–542.
- Rogers AE, Le JP, Sather S, et al. Mer receptor tyrosine kinase inhibition impedes glioblastoma multiforme migration and alters cellular morphology. *Oncogene.* 2012;31(38):4171–4181.
- Maheshwari G, Wiley HS, Lauffenburger DA. Autocrine epidermal growth factor signaling stimulates directionally persistent mammary epithelial cell migration. *J Cell Biol.* 2001;155(7):1123–1128.

36. Ivkovic S, Canoll P, Goldman JE. Constitutive EGFR signaling in oligodendrocyte progenitors leads to diffuse hyperplasia in postnatal white matter. *J Neurosci*. 2008;28(4):914–922.
37. Mellinghoff IK, Wang MY, Vivanco I, et al. Molecular determinants of the response of glioblastomas to EGFR kinase inhibitors. *N Engl J Med*. 2005;353(19):2012–2024.
38. Agarwal S, Sane R, Gallardo JL, Ohlfest JR, Elmquist WF. Distribution of gefitinib to the brain is limited by P-glycoprotein (ABCB1) and breast cancer resistance protein (ABCG2)-mediated active efflux. *J Pharmacol Exp Ther*. 2010;334(1):147–155.
39. Hofer S, Frei K. Gefitinib concentrations in human glioblastoma tissue. *J Neurooncol*. 2007;82(2):175–176.